



Investigation of Notch Root Strain Behaviors Under Combined Loadings

Toros Arda Aksen^{1*}, Emre Esener², Mehmet Firat¹

¹Sakarya University, Department of Mechanical Engineering, 54187, Esentepe/Sakarya, Turkey.

²Bilecik Seyh Edebali University, Department of Mechanical Engineering 11210, Gulumbe/Bilecik, Turkey. *Corresponding

*Author email: ardaaksen@sakarya.edu.tr

Abstract

Notches are the stress raiser regions. Along the notch section, not only the stress distribution becomes non-uniform, but also the stress level reaches the maximum value. These geometrical disorders can be undesirable such as casting cavity but sometimes these disorders are created deliberately for assembly process such as keyway holes or shaft steps. Because of the necessity of these notches. This is important to understand material behavior along this region.

In this study, three different strain paths were generated by the cyclic tensile and torsional loadings and strains of the notch root of a shaft which contains circumferential notch, were investigated through the finite element method (FEM). MSC. Marc commercial program have been used in this study as finite element software. The results have been obtained for kinematic hardening rules and compared with the experimental results obtained from literature studies. Also in this study, a subroutine file was used to calculate the Chaboche kinematic hardening rule parameters according to Swift equation.

Key words

Cyclic Plasticity, Kinematic Hardening, Finite Element Method

1. INTRODUCTION

The main purpose of this study is to investigate the notch root strains for circumferentially notched bar under the combined stress situation using FEM and also examine the effect of the back stress value for kinematic hardening. MSC.Marc software was used for finite element simulations. Strain paths were created through the tensile loadings and torsial loadings together.

There is a lot of similar studies in literature. Neuber [1] examined the shear stress distribution on sharp notched prismatic material subjected to shear loading and developed a mathematical model establishing relationship between elastic stress concentration factor, elastic – plastic stress factor and strain factor. Crews Jr. [2] investigated notch root stress and strains under the cyclic loadings by using Neuber and modified Stowell equations for different materials SAE 4130 and 2024-T3 aluminum alloy which had the same notch geometry. Barkey [3] developed a method for calculating the elasto-plastic strains at notch root under multiaxial loadings and compared the results with the finite element analyzes results. He recorded that the finite element results were compatible with experimental results. Hoffman [4] realized FE analysis of a shaft which has circumferential notch under incremental axial loading, bending moments. Koettgen [5] et al. used notch stress calculation method suggested by Hoffman and Seeger on a fatigue assessment of preloaded fuel injection pump and compared notch stress –strain results with elasto plastic FE analyzes.

Moftakhar [6] calculated notch stress – strain of filled and empty both two shafts using FE method under incremental axial loading and bending loads and he obtained suitable correlations. Firat [7] modeled circumferentially notched round bar and fulfilled FE analysis under combined axial and torsion loading and he compared notch root deformations with the notch root strain history. For both elastic and elastoplastic notch deformations, he obtained suitable results. Firat [8] also proposed simplified method related to stress – strain calculations at notch root under bending – torsion loads for fatigue life predictions. This method is based on the total strain energy density and he performed in phase, out phase cyclic loading simulations of SAE 1045 steel under combined bending – torsion loads according to constant amplitude. Critical plane based multiaxial damage assessments was fulfilled through Smith – Watson – Topper and Fatemi – Socie criteria. For both criteria, suitable cycle predictions were obtained in comparison with crack initiation cycles.

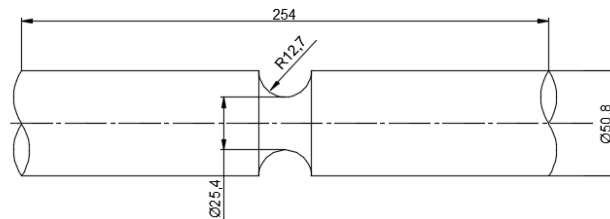


Figure 1. Circumferentially notched bar in 2D [3]

In this study, a circumferentially notched bar was modeled using Ansys software and the model was transferred to Marc finite element software. The dimensions of the circumferentially notched bar can be seen in Fig 1. Materials plastic properties were calculated according to Swift equation and the plastic parameters of the Swift equation were obtained from Hollomon parameters. In order to calculate materials plasticity parameters, a user subroutine file was used. This subroutine file requires Swift parameters for isotropic hardening solutions and besides the Swift parameters, saturation stress and saturation strain values for kinematic hardening solutions. So as to decrease solution time, because of the symmetry, half of the model was generated. Boundary condition of the half symmetric model can be shown in Fig 2.

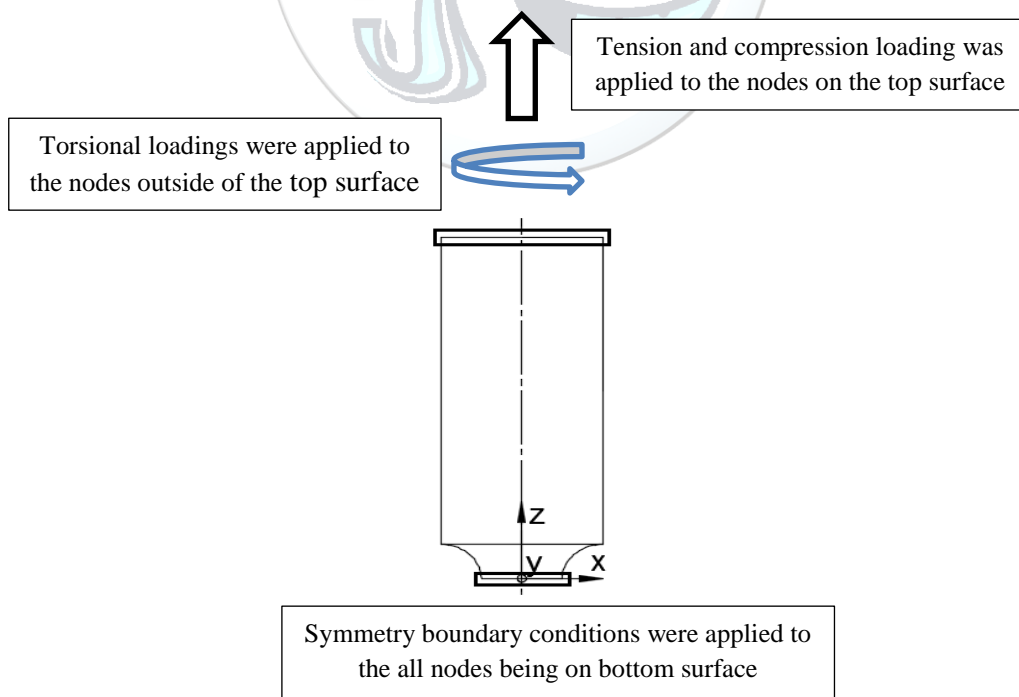


Figure 2. Boundary conditions applied on circumferentially notched bar in 2D

2. MATERIALS AND METHODS

2.1. Determination of Flow Curve

Material of the notched bar was determined as SAE1070 steel. The mechanical properties of SAE1070 steel were procured from the literature studies. The mechanical properties of the material are shown in Table 1.

Table 1. Mechanical properties of SAE1070 [3]

Parameter	Value
Young Modulus [MPa]	210000
Poisson Ratio	0,3
Yield Stress [MPa]	250
Cyclic Strength Coefficient [MPa]	1736
Cyclic Hardening Exponent	0,199

The stress values beyond the yield stress can be calculated according to power law equation shown in Eq. (1) [9].

$$\sigma_{\text{True}} = K \cdot \varepsilon_p^n \quad (1)$$

In the equation above, K is the strength coefficient, n is the strain hardening exponent. Plastic strain which is expressed as ‘‘ ε_p ’’ can be calculated by the following equation.

$$\varepsilon_p = \varepsilon_T - \frac{\sigma_{\text{True}}}{E} \quad (2)$$

In this study, materials plastic parameters were calculated according to Swift equation and in order to obtain Swifts parameters, curve fitting method was implemented in Excel program. The flow curve obtained from the Hollomon power equation was matched with the Swift’s equation. According to Swift’s equation, true stress beyond the yield strength can be expressed by the following equation [9].

$$\sigma_{\text{True}} = C \cdot (\varepsilon_0 + \varepsilon_p)^p \quad (3)$$

In Swift equation, C is the strength coefficient, p is the hardening exponent. To determine these parameters, curve fitting was applied and strength coefficient was obtained as 1800 MPa, hardening exponent was obtained as 0,215.

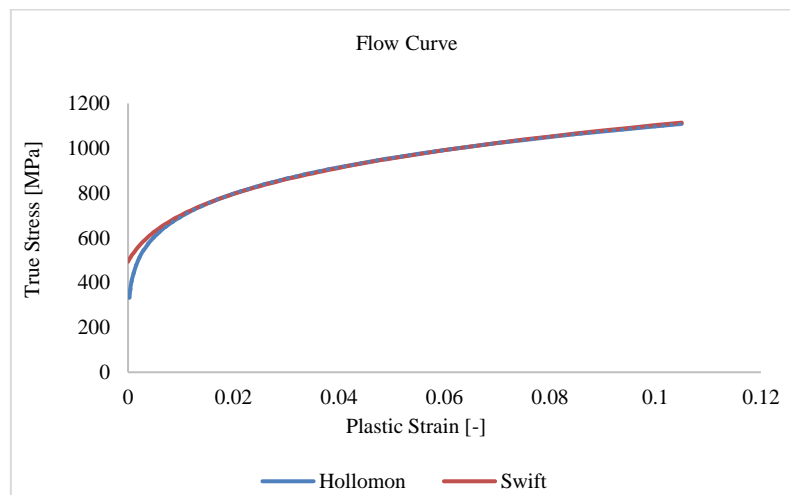


Figure 3. Curve fitting for Swift parameters

Along with the yield criteria and flow rule, hardening rule is required to define plasticity. Hardening rules describe the change of the yield surface and can be disintegrated into isotropic hardening and kinematic hardening rules. Backstress concept is associated with the kinematic hardening rule. Armstrong and Frederick expressed the backstress tensor increment as following equation [7], [8].

$$d\underline{\underline{\alpha}} = \frac{2}{3} C d\underline{\underline{\epsilon}}^p - \gamma \underline{\underline{\alpha}} dp \tag{4}$$

In Eq. (4), C and γ are the material constants; $d\underline{\underline{\epsilon}}^p$ and dp are the plastic strain tensor and equivalent plastic strain increment respectively. Chaboche and Rousselier disintegrated the back stress tensor into few parts which has different hardening properties. It is assumed that 5 parts will be adequate to calculate the plastic part of the material [7], [8], [10], [11], [14], [15].

$$\underline{\underline{a}} = \sum_{i=1}^n \underline{\underline{a}}^{(i)} ; \quad i = 1, 2, \dots, m \tag{5}$$

$$d\underline{\underline{\alpha}}^{(i)} = \frac{2}{3} C^{(i)} d\underline{\underline{\epsilon}}^p - \gamma^{(i)} \underline{\underline{\alpha}}^{(i)} dp \tag{6}$$

‘i’ represents the arbitrary partition number which the back stress was divided. Equivalent plastic strain increment can be expressed as following inequality [7], [16].

$$0 \leq dp^{(i)} \leq \sqrt{\frac{2}{3} \underline{\underline{\epsilon}}^p \underline{\underline{\epsilon}}^p} \tag{7}$$

Jiang and Sehitoglu proposed another kinematic hardening model and define the backstress tensor increment as following equation [7], [14].

$$d\underline{\underline{\alpha}}^{(i)} = c^{(i)} \cdot r^{(i)} \cdot \left[\underline{\underline{n}} - \left(\frac{\|\underline{\underline{\alpha}}^{(i)}\|}{r^{(i)}} \right)^{\chi+1} \cdot \underline{\underline{L}}^{(i)} \right] \cdot dp ; \quad i = 1, 2, \dots, m \tag{8}$$

Here $c^{(i)}$, $r^{(i)}$ and $\chi^{(i)}$ are the scalar parameters; L is the unit tensor of the back stress tensor which can be expressed as following equation [7].

$$\underline{\underline{L}}^{(i)} = \frac{\underline{\underline{\alpha}}^{(i)}}{\|\underline{\underline{\alpha}}^{(i)}\|}; \quad (i = 1, 2, \dots, m) \tag{9}$$

$\underline{\underline{n}}$ is the unit tensor of the yield surface normal which belongs to the related stress point and expressed by Eq. (10) [7], [12], [17].

$$\underline{\underline{n}} = \frac{\underline{\underline{S}} - \underline{\underline{\alpha}}}{\|\underline{\underline{S}} - \underline{\underline{\alpha}}\|} \tag{10}$$

Yield surface is the limit which the material can endure without exposed to any plastic deformation and can be define by following equation [7], [12].

$$F = \|\underline{\underline{S}} - \underline{\underline{\alpha}}\| - \sqrt{\frac{2}{3}} \cdot \sigma_0 \tag{11}$$

In Eq. (11), $\underline{\underline{S}}$ is the deviatoric stress component. According to the consistency condition, yield surface remains steady during plastic deformation as expressed in Eq. (12) [7] [12].

$$dF = 0 \tag{12}$$

Additionally, consistency condition can be expressed as Eq. (13).

$$d\underline{\underline{S}} : \underline{\underline{n}} - d\underline{\underline{\alpha}} : \underline{\underline{n}} = 0 \tag{13}$$

Plastic hardening modulus can be defined by Eq. (14).

$$h = \frac{d\underline{\underline{\alpha}} : \underline{\underline{n}}}{dp} \tag{14}$$

Through substituting Eq. (8) and Eq. (14), hardening modulus may be expressed as following equation [7], [12].

$$h = c^{(i)} r^{(i)} \left(1 - \left(\frac{\|\underline{\underline{\sigma}}^{(i)}\|}{r^{(i)}} \right)^{\chi^{(i)+1}} \right) \underline{\underline{I}}^{(i)} : \underline{\underline{n}}; \quad (i = 1, 2, \dots, m) \quad (15)$$

$c^{(i)}$, $r^{(i)}$ which are also known as Jiang parameters can be calculated according to the following equations [7], [10], [11], [12], [14], [15].

$$c^{(i)} = \sqrt{\frac{2}{3}} \cdot \frac{1}{\varepsilon_a^{(i)}}; \quad i = 1, 2, \dots, m \quad (11)$$

$$r^{(i)} = \frac{2}{3} \cdot \frac{H^{(i)} - H^{(i+1)}}{c^{(i)}}; \quad i = 1, 2, \dots, m \quad (12)$$

In the Eq. (12), H represents the slope between two points in sequence which belong to the stabilized cyclic stress – strain curve [7]. These points have to be selected between yield stress and ultimate tensile stress. Slope of the curve can be calculated according to Eq. 13 [7], [12].

$$H^{(i)} = \frac{\sigma_a^{(i)} - \sigma_a^{(i-1)}}{\varepsilon_a^{(i)} - \varepsilon_a^{(i-1)}}; \quad i = 1, 2, \dots, m \quad (13)$$

Hardening slope which belongs to the last point is zero. Other initial conditions are described in Eq. (14) [7], [10], [11], [12].

$$\sigma_a^{(0)} = 0; \quad \varepsilon_a^{(0)} = 0; \quad H_{(m+1)} = 0 \quad (14)$$

2.2. Finite Element Method

The model was generated in Ansys software. The coordinate systems of the nodes were transferred from the cartesian to cylindrical coordinate system and the boundary conditions were regulated for cylindrical coordinate system in Ansys. Then the model was transferred from Ansys to Marc software. Element density at the notch root was increased toward to the specimen surface because it is assumed that the stress level will reach the maximum level on surface.

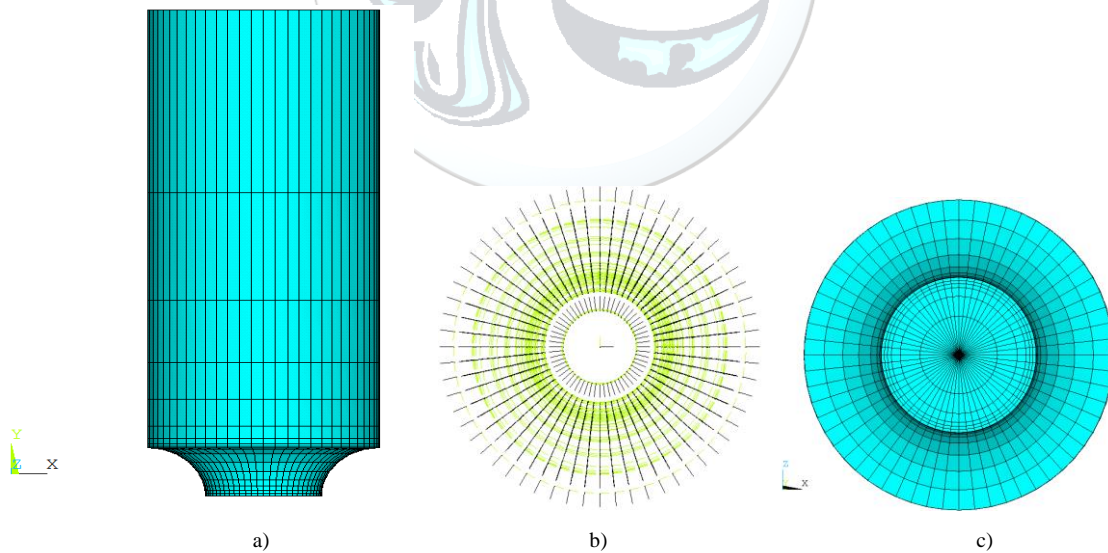


Figure 4. a) Model created through Ansys software. b) Cyl. coord. sys. of the nodes. c) Bottom view of the model.

In Fig. 5, green line represents Θ axis which is transformed from the y axis and black line represents the r axis which is transformed from the x axis. Also there is z axis in cylindrical coordinate system which is perpendicular to the $r - \Theta$ plane. The notched bar model transferred to Marc software can be seen in Fig 5.

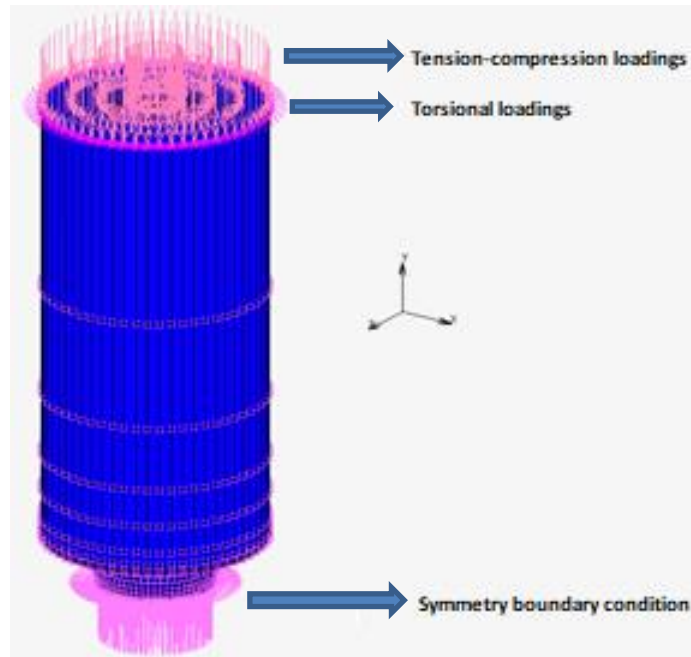


Figure 5. Model transferred to Marc software

2.2.1. Boundary Conditions

There strain paths which contain torsional and cyclic tension-compression loadings, were applied to the notched shaft. These strain paths are proportional loading, box type non-proportional loading and zig-zag type non-proportional loading, Strain paths can be shown in Fig 6.

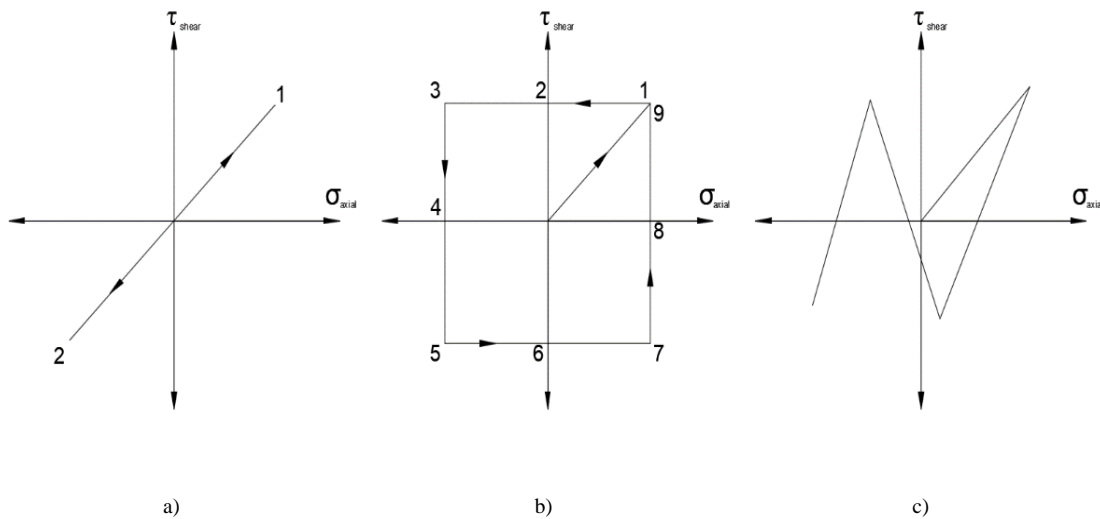


Figure 6. a) Proportional loading, b) Box type non-proportional loading. c) Zig-zag type non-proportional loading [3], [7]

The stress occurred at the notch root is determined according to the nominal stress defined by Barkey. The nominal stresses created at the notch root can be seen in following table.

Table 2. Nominal stresses created at the notch root [3], [7]

Test Number	Nominal Axial Stress [MPa]	Nominal Shear Stress [MPa]	Loading Condition
1	296	193	Proportional Loading
2	296	193	Non-proportional Loading (Box)
3	296	193	Zig – Zag Type Loading

Because of the stress concentration at the notch root, the stress level reach the maximum level which is much more than the nominal stress. So, stress values in table 2 represent the stresses calculated at the notch root according to geometrical dimensions regardless of plastic deformation and stress concentration.

2.2.2. Subroutine File Regulations

A subroutine file called as Hypela 2 was used in this study for calculating the kinematic hardening rule parameters. In order to regulate the isotropic hardening parameters, in addition to the Young Modulus, Poisson ratio and yield stress, Swift parameters should be entered to the subroutine file. Besides the isotropic parameters, back stress components which are saturation stress and saturation strain data were entered to this subroutine file. Analyzes according to kinematic hardening rule assumptions were realized. To predict the accurate back stress parameters certain analyzes were performed in rows. First back stress parameters are determined by offsetting the flow curve to below as yield stress and the saturation stress value determined as 855 MPa for saturation strain equal to 0,1. According to the deviations and the convergence to the experimental results, the back stress parameters were updated at every turn until the appropriate results were obtained. The first saturation stress and saturation strain values obtained from the flow curve can be shown in Fig 7.

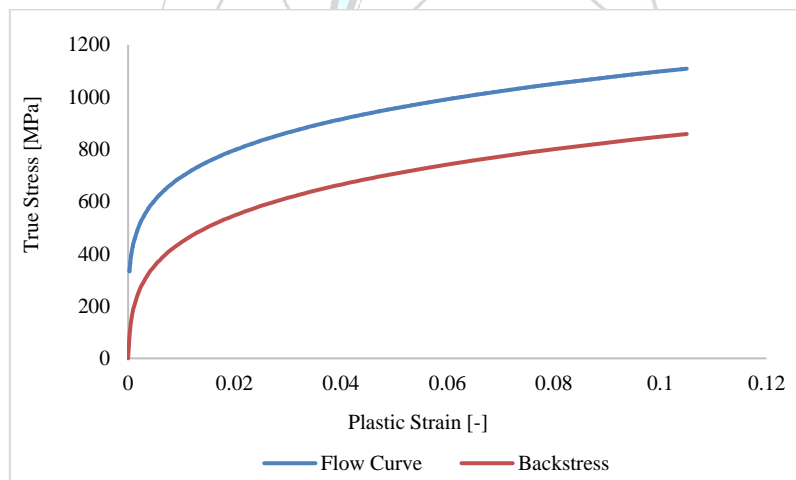


Figure 7. Saturation stress and saturation strain values obtained from the flow curve

3. RESULTS AND DISCUSSION

In order to examine strain behavior, a node which is located at the notch root, on the surface of the bar was examined. The results were compared with the experimental outcomes obtained by Barkey [3]. The results under proportional loadings can be shown in following Fig 8 for different saturation stresses.

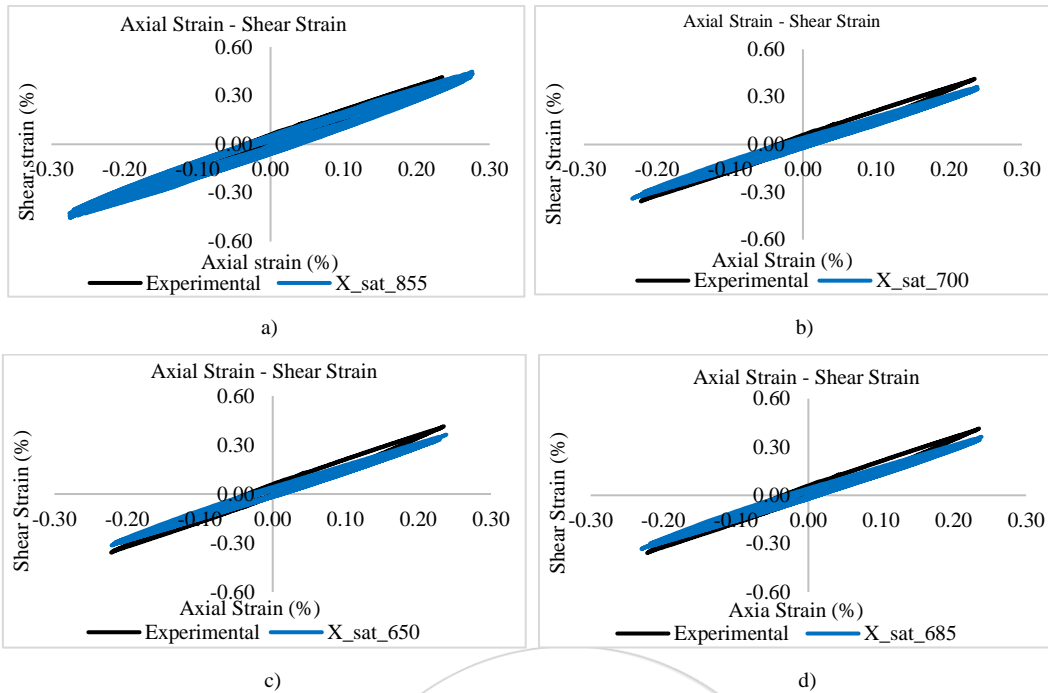


Figure 8. Axial strain – shear strain results under proportional loadings. a) Saturation stress 855 MPa, b) Saturation stress 700 MPa, c) Saturation stress 650 MPa, d) Saturation stress 685 MPa

The results under the box type non-proportional loadings can be shown in Fig 9 for different saturation stresses.

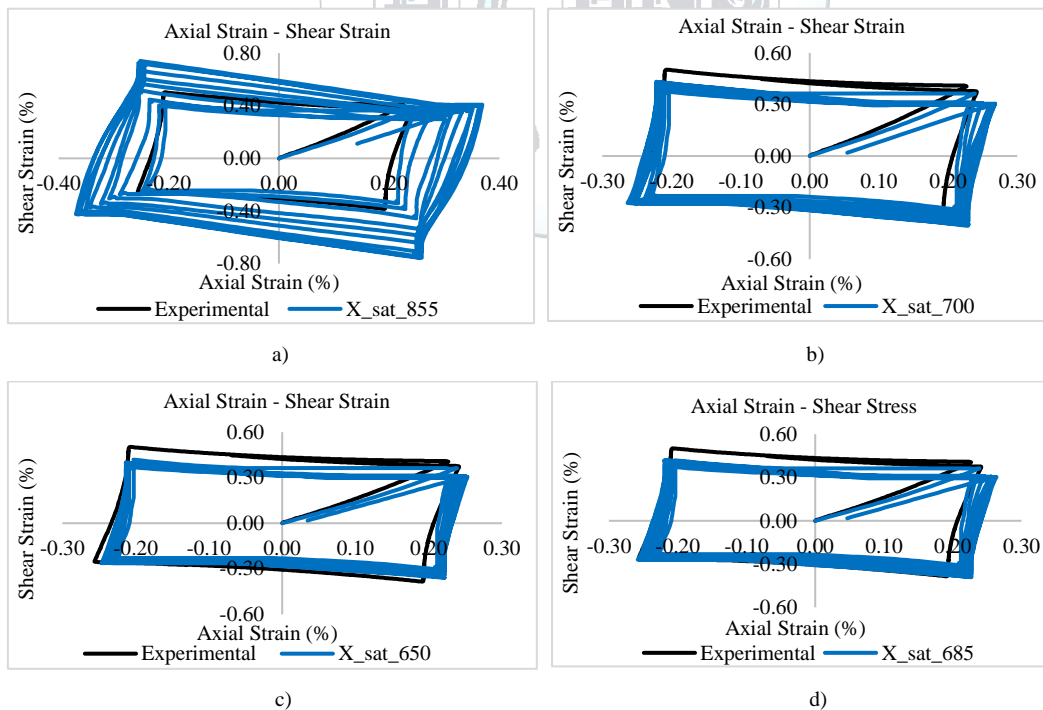


Figure 9. Axial strain – shear strain results under box type non-proportional loadings. a) Saturation stress 855 MPa, b) Saturation stress 700 MPa, c) Saturation stress 650 MPa, d) Saturation stress 685 MPa

The results under the zig-zag type non-proportional loadings can be shown in Fig 10 for different saturation stresses.

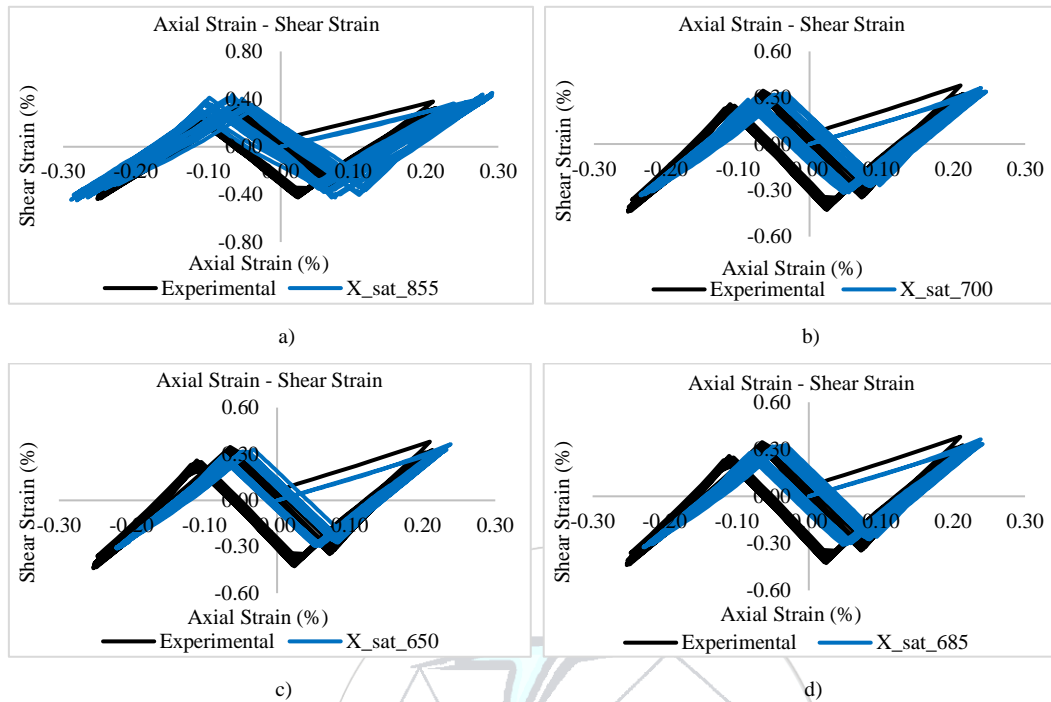


Figure 10. Axial strain – shear strain results under zig-zag type non-proportional loadings. a) Saturation stress 855 MPa, b) Saturation stress 700 MPa, c) Saturation stress 650 MPa, d) Saturation stress 685 MPa

4. CONCLUSION

In this study, under the combined loadings, notch root strain behaviors of a circumferentially notched bar were investigated. These combined loadings were proportional loadings, box type non-proportional loadings and zig-zag type non-proportional loadings. Analysis were performed according to the kinematic hardening rule assumptions. To define the kinematic hardening rule parameters, a user subroutine file was used and the plasticity calculations were realized according to Swift equation. Swift parameters were obtained from the Hollomon parameters which were procured from the literature studies. In order to calculate the back stress, saturation stress values were updated repeatedly. Then the solutions were compared with the experimental results.

It can be seen that the results were in accord with the experimental data. For all loading types, this is similar that, the results obtained according to 855 MPa saturation value, showed deviations in comparison with the experiments. Then the saturation stress values were updated to 700 MPa, 650 MPa and 685 MPa respectively. The results were close to each other and the deviations were fell off. For the results obtained according to the 650 MPa saturation stress, deviations were the lowest but the results diverged from the experimental results. The optimal results were obtained according to the saturation stress equal to the 685 MPa because the outcomes were in accord with the experimental results and the deviations were lower. In addition, calculating the strain behaviors at notch root according to the different back stress values is difficult and time consuming process. In this study this process accomplished readily through a user subroutine file.

REFERENCES

- [1]. H. Neuber, "Theory of stress concentration for shear strained prismatic bodies with arbitrary stress – strain law," *Journal of Applied Mechanics*, vol 28, pp. 544-550, Dec. 1961.
- [2]. H. J. Crews, "Elastoplastic stress – strain behaviour at notch roots in sheet specimens under constant – amplitude loading," Langley Research center, NASA Technical Report, D-5253, 1969.

- [3]. Barkey, M., E., "Calculation of notch strains under multiaxial nominal loading," Ph.D. thesis, University of Illinois, College of Engineering at Urbana-Champaign, Oct. 1993.
- [4]. M. Hoffmann, "Ein naeherungsverfahren zur ermittlung mehrachsiger elastisch-plastischer kerbeanspruchungen", M.Eng thesis, Darmstadt Technical University, Germany, 1985.
- [5]. V.B. Koettgen, M. Schoen, and T. Seeger, "Application of multiaxial load notch strain approximation procedure to autofrettage of pressurized components," *American Society for Testing and Materials*, pp. 375-396, 1993.
- [6]. A.A. Moftakhar, "Calculation of time – independent and time – dependent strains and stresses in notches," M.Eng. thesis, University of Waterloo, 1994.
- [7]. M.Firat, "Cyclic plasticity modeling and finite element analysis of a circumferentially notched round bar under combined axial and torsion loadings", *Material and Design*, vol. 34, pp 842-852, Feb. 2012.
- [8]. M. Firat, "A numerical analysis of combined bending – torsion fatigue of SAE notched shaft," *Finite Elements in Analysis and Design*, vol. 54, pp. 16-27, 2012.
- [9]. G. E. Dieter, *Mechanical Metallurgy*, SI metric ed., United Kingdom, 1988.
- [10]. M. Firat, U. Kocabicak, "Analytical durability modeling and evaluation – complementary techniques for physical testing of automotive components," *Engineering Failure Analysis*, vol. 11, pp. 655–674, 2004.
- [11]. M. Firat, U. Kocabicak, "A simple approach for multiaxial fatigue damage prediction based on FEM post-processing," *Materials and Design*, vol. 25, pp. 73–82, 2003.
- [12]. M.Firat, "U-channel forming analysis with an emphasis on springback deformation," *Material and Design*, vol. 28, pp 147-154, Feb. 2007.
- [13]. Y. K. Lin, K. M. Hsu and P.K. Lee, "The application of flow stress flow stress model to sheet metal forming simulation," *Iron & Steel Research & Development Department, China Steel Technical Report*, No 23, pp.31-35, 2010.
- [14]. Y. Jiang and H. Sehitoglu, "Modeling of cyclic ratcheting plasticity, part I: development of constitutive relations," *Journal of Applied Mechanics*, vol. 63, pp. 720-725, Sept 1996.
- [15]. Y. Jiang and H. Sehitoglu, "Modeling of cyclic ratcheting plasticity, part II: comparison of model simulations with experiments," *Journal of Applied Mechanics*, vol. 63, pp. 726-733, Sept 1996.
- [16]. N. Ohno and J. D. Wang, "Kinematic hardening rules with critical state of dynamic recovery, part I: formulation and basic features for ratcheting behavior", *International Journal of Plasticity*, vol. 9, pp. 375-390-650, 1993.
- [17]. J. Lemaitre and J. L. Chaboche, "Mechanics of Solid Materials", Cambridge University Press, New York, 1990.

